NBactSPACE

Easily up-scalable and non-toxic coatings with antimicrobial broad spectrum activity for spacecraft indoors

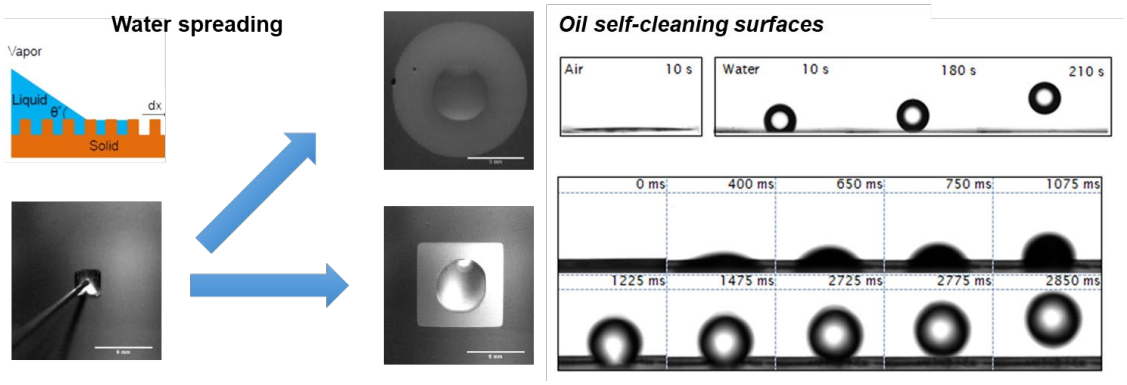

Ref. ESA	**Contract N° ESA AO/1-9363/18/NL/KML** "Materials for antimicrobial / antifungal surface treatment in confined inhabited environment in human spaceflight."
Ref. LIST	NBactSPACE / Executive Summary Report 211119
Subject	Concise summary of the findings of the Contract
Date	November 19th, 2021

Issue	Date	Comments
1	19/11/2021	Initial issue

Distribution List

Receiving Entities	Copies
ESA Malgorzata Holynska Johannes Witt Rob Postema Cathal Mooney Mauricio Portaluppi Viktorija Piaulokaite Christel Paille Pierre Rebeyre Christophe Lasseur Raul Alarcon Riccardo Rampini Yuriy Butenko Michal Malicki Olivier Perat	
LIST (internal distribution) Nikolaos Gomopoulos All NBactSpace participants	Share folder

Table of Contents

Documents

Applicable Documents

[AD01]	App.1 to AO/1-9363/18/NL/KML	Statement of Work; ESA Express Procurement Plus - EXPRO+: Materials for antimicrobial / antifungal surface treatment in confined inhabited environment in human spaceflight, Reference ESA-TECQEE-SOW-009636 Issue 2 Revision 3 Date of Issue 22/05/2018
[AD02]	MRT/NBacSPACEv181012	Project proposal
[AD03]	REACH	REACH candidate List of substances of very high concerns for Authorization (http://echa.europa.eu/candidate-list-table)
[AD04]	ISS MORD	International Space Station Medical Operations Requirements Document (ISS MORD), SSP50260 Rev. E, November 2017

Reference Documents

Proposal in response to ESA ITT N°AO 9363: MRT/NBactSPACE v181012
NBactSPACE - Minutes of PM3WP3 v200210
NBactSPACE - Minutes of PM2WP3 v191210
NBactSPACE - Minutes of PMWP3 v191001
NBactSPACE - Minutes of RWP2 v190730
NBactSPACE - Minutes of RWP1 v190516
NBactSPACE - Minutes of PR1 v190326
NBactSPACE - Minutes of R1 v190502
NBactSPACE – Plan of manufacture of 5 LIST solutions TN2.1 v190705
NBactSPACE - Minutes of progress meeting 2 v 190715
COL-RIBRE-TN-1332 v970212
ISO 10993 part 5
ISO 10993 part 12
ASTM G85 – 09
BS EN 16105:2011
[RD01] ECSS-E-ST-32-08C Rev.1 Materials
[RD02] ISO22196:2011/JIS Z 2801, Measurement of antibacterial activity on plastics and other non-porous surfaces. https://www.iso.org/standard/54431.html
[RD03] ECSS-Q-ST-70C Rev.1 Materials, mechanical parts and processes
[RD04] ESA Contract No. 4000120584/17/NL/KML/md - New Material for Water Condensate – State of the Art Review on the Design of Antimicrobial Surfaces. TN1.1
[RD05] ESA Contract No. 4000120584/17/NL/KML/md - New Material for Water Condensate –State-of-the Art Review on Methodologies / Standards for Characterisation of Antimicrobial Surfaces. TN1.2
[RD06] ECSS-Q-ST-70-29C Determination of offgassing products from materials and assembled articles to be used in a manned space vehicle crew compartment
[RD07] ECSS-Q-ST-70-17C Durability testing of coatings (1 February 2018)
[RD08] MRT/NBactSPACE /TN1.1/190507 NBactSpace, Review of existing antimicrobial coatings
[RD09] MRT/NBactSPACE /TN1.2/190507 NBactSpace, Specification of detailed requirements
[RD10] MRT/ NBactSPACE / TN3.2 200313 NBactSpace, Full test plan
[RD11] MRT/NBactSPACE / Technical note 3.1 Results of preliminary screening
[RD12] MRT/NBactSPACE / Technical note 4.1 Results of tests on optimized samples
[RD13] MRT/NBactSPACE / Technical note 4.2 Full test plan
[RD14] Chowdhury, S., Y. L. Teoh, K. M. Ong, N. S. Rafflisman Zaidi, and S. K. Mah. 2020. Poly(Vinyl) alcohol crosslinked composite packaging film containing gold nanoparticles on shelf life extension of banana. Food Packaging and Shelf Life 24:100463
[RD15] MRT/NBactSPACE / Technical note 5.2 Results of tests on up-scaled samples

Acronyms

ToF-SIMS	Time-of-Flight secondary ion mass spectrometry
XPS	X-Ray Photoelectron Spectroscopy
SEM	Secondary electron microscopy
AFM	Atomic force microscopy
PVA	Poly (vinyl alcohol)
PAA	Poly (acrylic acid)
CNC	Cellulose nanocrystal

DOE	Design of experiment
HIM	Helium ion microscopy
PEI	Poly (ethylene imine)
GO	Graphene oxide
PBS	Phosphate buffer solution
HMDSO	HexaMethylDiSilOxane

1 INTRODUCTION

The occurrence of infectious diseases inside inhabited manned spacecrafts is considered as a serious threat for the success of future spatial missions, more particularly since the recent discoveries of the first antibiotic-resistant pathogens in the ISS at the end of 2018. At the same time, the immune system of astronauts is altered, making the occurrence of infectious diseases easier. In order to decrease the risk of infectious disease due to the formation of biofilms on indoor spacecraft surfaces and suits, the deposition of antimicrobial coatings combined with the surface cleaning with dry cleansing products is the most suitable approach. Several commercial antimicrobial coatings are already accessible on the market for terrestrial conditions and with a cytotoxicity level still acceptable for commercial use. However, the future regulations on the use of chemicals (REACH) and the confined conditions on inhabited spacecraft makes most of these solutions non relevant for inhabited spacecrafts. A new generation of coatings, safer for the crews, needs to be developed. A very few safe by design coatings are commercialized but their antimicrobial efficiency is still low, or their durability is limited. In this summary, we will present the findings obtained for the different LIST coatings, fabricated in WP3, WP4 and WP5.

2 METHODOLOGY

The most important results are presented by LIST coatings developed in the NBACTSPACE project, in a chronological order. They are discussed relatively to the state-of-the-art and the commercial references tested in this project. The findings concern mainly the antimicrobial effect, cytotoxicity, durability, adhesion, wettability, ageing and off-gassing.

3 WP3-SOLUTION 1: METHACRYLATE-BASED ATMOSPHERIC PECVD AND SURFACE GRAFTING OF PEPTIDE

LIST WP3-solution 1 is based on the application of atmospheric-pressure dielectric barrier discharge plasmas to polymerize methacrylate monomers to deposit crosslinked, water stable and highly chemically reactive interlayers (Figure 1). This intermediate layer ensures a rapid and selective covalent immobilization of biomolecules by the introduction of a L-DOPA-based specific linker within the macromolecular structure.
In the same plasma reactor, the surface is firstly cleaned/activated by oxygen plasma. After, the plasma deposition is done by cyclic sequencing of the application of a very thin liquid layer of the monomer mixture (ethylene glycol dimethacrylate and L-DOPA methacrylamide) over the whole substrate surface by means of a nebulization system and a moving table, followed by the exposure of this thin liquid layer to argon plasma (Figure 1). The process is repeated until the coating reach its optimal thickness. The as-prepared plasma coated surfaces is then immersed in PBS buffer solutions containing the antimicrobial peptide to carry out the covalent immobilization of the biomolecules by reaction with the catechol/quinone groups introduced on the methacrylic layer by L-DOPA-derived co-monomer.
The as-deposited plasma layer is characterized by its hydrophilicity (WCA= 50°), smoothness (RMS<40 nm, by AFM) and stability in water and buffer liquid medias (immersion tests). In addition, it is resistant to common sterilization procedures (UV, ethanol, autoclave etc).

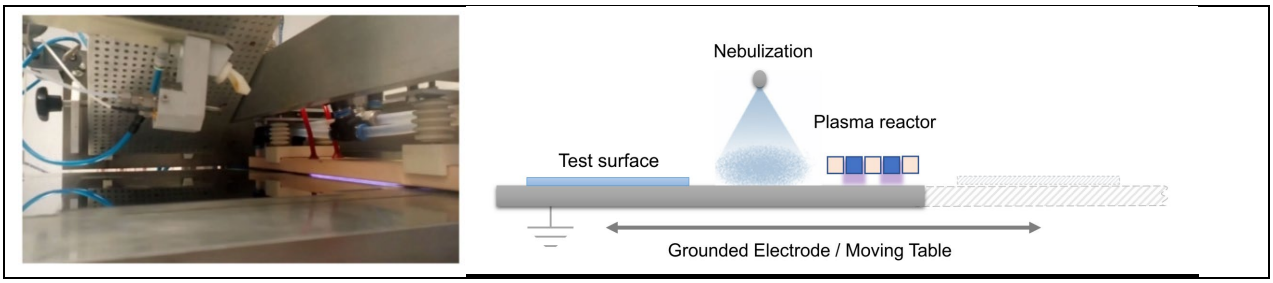

Figure 1. Atmospheric-pressure plasma polymerization setup developed at LIST for large area surfaces and the schematic representation of its fundamental parts

XPS characterization indicated a N at.% content of 5-6% indicating the presence of the monolayer of lysozyme, the antimicrobial peptide selected. ToF-SIMS analyses validate the presence of this monolayer of lysozyme.

Unfortunately, no antibacterial nor antifungal effect is detected with this plasma coating. To check if the nature of the antimicrobial peptide, lysozyme, was the reason for this surprising result, we replaced this antimicrobial peptide by another one called glucose oxidase, supposed to have a different selectivity for pathogen inactivation. Again, no antibacterial, nor antifungal effect is detected. These results indicate that the use of antimicrobial peptide is not trivial. First, they are active against specific pathogens. A need for several antimicrobial peptides is therefore mandatory to get a broad-spectrum antimicrobial effect, making the deposition process complicated. Second, an optimized density and orientation of the antimicrobial peptide molecules is mandatory to get a significant antimicrobial effect. Again, it is not easy to reach these optimal conditions. Therefore, with the knowledge available today, it seems to be an approach difficult to implement at the industrial scale.

4 WP3-SOLUTION 2: HMDSO-BASED ATMOSPHERIC PECVD HYDROPHOBIC COATING

LIST WP3-solution 2 is based on the application of atmospheric-pressure dielectric barrier discharge plasmas to polymerize HMDSO to deposit crosslinked, water stable and hydrophobic coatings by using the same system presented above but without the nebulizer (Figure 1). Indeed, HMDSO can be easily vaporized at atmospheric pressure.
The surface is firstly cleaned/activated by oxygen plasma. After, the plasma deposition is done by passing the plasma electrode several time above the substrate to reach the targeted thickness around 100 nm.
The as-deposited plasma layer is characterized by its hydrophobicity (WCA= 90°), smoothness (RMS<20 nm, by AFM) and stability in water and buffer liquid medias (immersion tests). In addition, it is resistant to common sterilization procedures (UV, ethanol, autoclave etc).
XPS analyses, that are specific to the extreme surface, indicates an organic character (44% at. C) and a significant content of N (4 % at. N) embedded in the coating due to the reaction of plasma activated air with the precursor. Looking more carefully at the nature of bonds at the extreme surfaces (0 to 10 nm from surface) with XPS, it shows that most of the C atoms are bound to C or H atoms (alkyl) and 10-20% are bound to O and some N. Si is mainly bound to 2 O and 2 C in average similarly to PDMS. O is linked to both C and Si.
As shown on Figure 2 (left, red rectangle), antimicrobial tests following the procedure **ISO 22196:2011** indicates a limited effect on G- bacteria *E. coli* (1.5-2 log reduction) and no antibacterial effect against G+ bacteria *S. aureus* nor antifungal effect against *A. niger*. Antimicrobial properties observed on *E. coli* could come from free radicals trapped in the coatings or some N-containing chemical groups formed in coatings due to the plasma process. This is an interesting result because this surface contact killing effect is combined to a hydrophobic surface and a simple chemistry. Finally, the HMDSO-based plasma hydrophobic coatings did not show any cytotoxicity on keratinocytes after 48h with the LDH assay (Figure 2, right, orange bars). This coating passed all the durability tests. In conclusion, it is an interesting approach, but the antimicrobial efficiency has to be improved by, for example, adding an additional antimicrobial agent or by patterning the coating or the substrate.

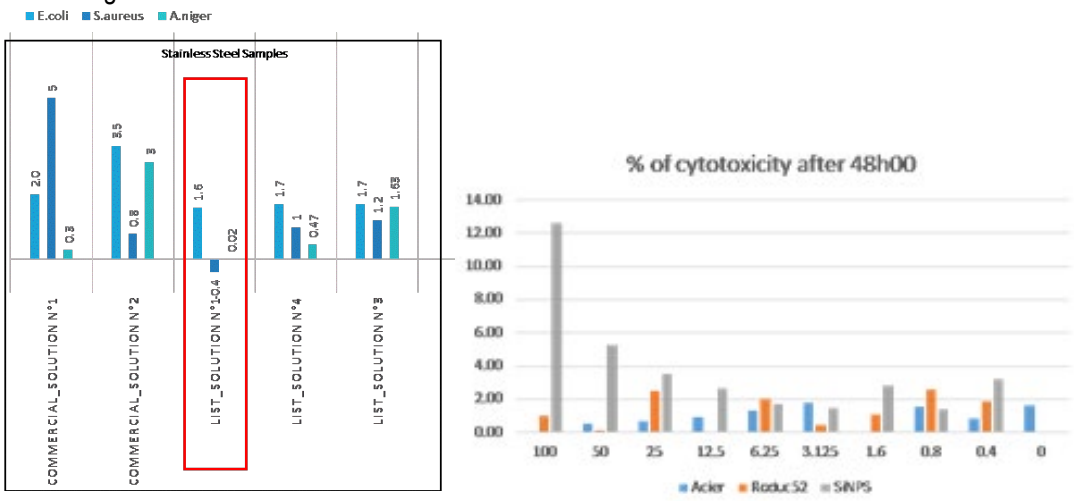

Figure 2. (left) Inside the red rectangle, antimicrobial Activity, R *(logarithm reduction of the number of surviving micro-organisms in cells/cm2)* of antimicrobial HMDSO-based hydrophobic coatings deposited on stainless steel for *E. coli* (left), *S. aureus* (center) and *A. niger* (right); (right) Cytotoxicity (%) on human skin keratinocytes cells with the LDH assay on HMDSO-based hydrophobic plasma coatings (in orange).

5 WP3-SOLUTION 3: PVA-based coatings embedding lignin nanoparticles

The idea here is to combine the effect of several natural-based antimicrobial agents such as Kraft lignin and chitosan inside a biocompatible polymer matrix. To improve the antimicrobial effect of the lignin and the retention of the lignin in the coating, lignin molecules are structured as nanoparticles. LIST wet solution 3 methodology is based on the deposition of a liquid formulation by dip-coating, spin-coating or bar coating and a thermal treatment to evaporate the solvent and cross-linked the PVA with boric acid, that can also play an antimicrobial role (Figure 3). The PVA cross-linked structure can allow a good compromise between mechanical strength and chemical stability. These PVA-based coatings have been already tested for their durability and PVA is suitable for biomedical applications.

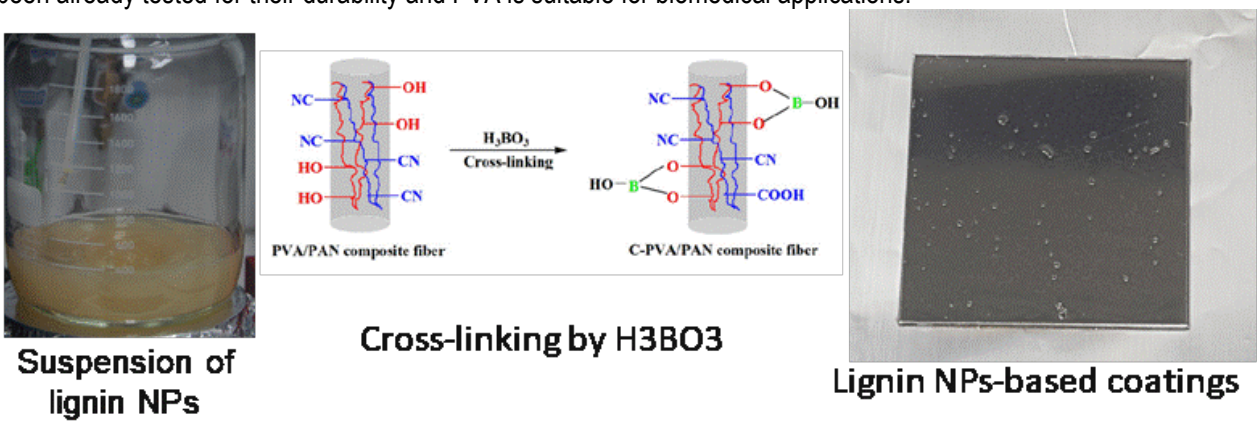

Figure 3. Fabrication of PVA-based coatings embedding lignin nanoparticles

Kraft lignin nanoparticles are fabricated in LIST using a solvent shifting approach. Then, an aqueous solution of chitosan, polyvinyl alcohol (PVA), boric acid (H3BO3) is prepared first. Boric acid is used to cross-link the PVA. Then, this solution is mixed with the lignin nanoparticle suspension. The mixture of polyvinyl alcohol, boric acid, chitosan and lignin nanoparticles is applied on the substrates by dip-coating on steel and polyimide substrates. Polyethylene imine (PEI) is added prior to deposition to improve the adhesion of the coatings. A curing in an oven at 110°C for 2h was used to dry the applied mixture and to cross-link the final coatings (Figure 3).

Chemical analyses by ToF-SIMS spectra show the presence of PVA and boric acid. Chitosan is not detected. XPS confirms these results and show a content of 1 at. % B in the coatings. Therefore, antimicrobial effects are mainly due to boric acid and to a lower extent lignin nanoparticles and chitosan. Chitosan can also have an effect even if present in low quantity as it is interacting more strongly with the pathogen cell walls, allowing lignin and boric acid to better interact/penetrate inside the pathogen cells. WCA measurements show a slightly hydrophilic behaviour with a WCA around 55°. These coatings show a strong antibacterial effect on both G- bacteria *E. coli* (3 log reduction) and against *S. aureus* (4 log reduction) when deposited on kapton with a concentration of 0.15 w.% (Figure 4). The antibacterial effect is lower for G+ *S. aureus* when deposited on Kapton with a lower lignin nanoparticles concentration of 0.015 w.%. The antibacterial effect is lower for G+ *S. aureus* and G- *E. coli* when deposited on stainless steel even with the higher concentration of lignin nanoparticles of 0.15 w.% (Figure 4). It appears that a higher lignin nanoparticles content of 0.15 w.% is needed to inhibit G+ *S. aureus* bacteria proliferation. The lower antibacterial effect observed on stainless steel is probably due to the fact that less bacteria can grow/survive on the reference non-coated stainless steel compared with non-coated kapton foils due to the presence of Cr in the stainless steel composition.

The most important finding here is the strong antifungal effect on *A. niger* (1.1-1.6 log reduction) when deposited on both stainless steel and polyimide (Kapton) with a concentration in lignin of 0.15 w.%. No antifungal effect is detected on *A. niger* when deposited on Kapton with a lower lignin nanoparticles concentration of 0.015 w.%. (Figure 4). For *A. niger*, it appears that a higher lignin nanoparticles content of 0.15 w.% is needed to inhibit *A. niger* fungi proliferation. The lower antifungal effect observed on kapton is probably due to the fact that less fungi can grow/survive on the reference non-coated kapton foils compared with non-coated stainless steel coupons.

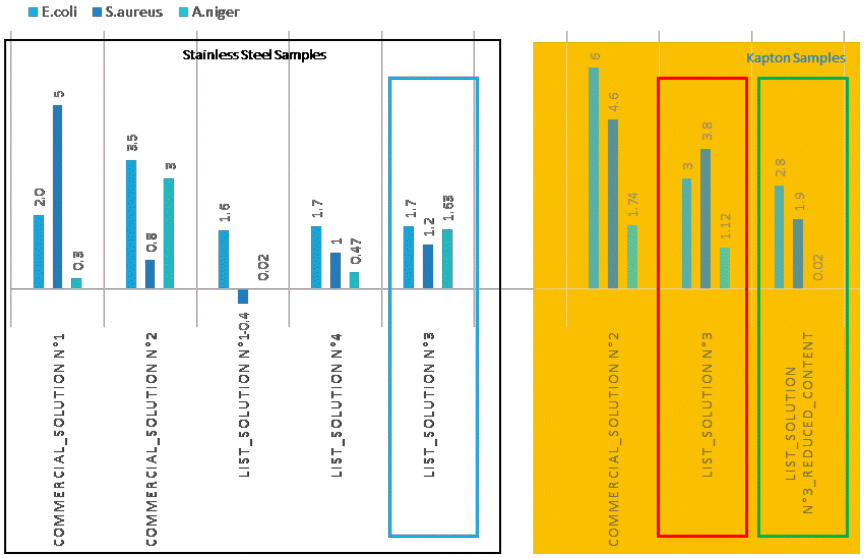

Figure 4. Antimicrobial Activity, R *(logarithm reduction of the number of surviving micro-organisms in cells/cm2)* of PVA-based coatings embedding lignin nanoparticles for *E. coli* (left column), *S. aureus* (center column) and *A.niger* (right column). Inside blue rectangle, the PVA-based coatings embedding lignin nanoparticles (0.15 w.%) deposited on stainless steel; inside red rectangle, the PVA-based coatings embedding lignin nanoparticles (0.15 w.%) deposited on polyimide (Kapton), and in green rectangle, the PVA-based coatings embedding lignin nanoparticles (0.015 w.%) deposited on polyimide (Kapton)

When deposited on stainless steel, PVA-based coatings embedding lignin nanoparticles (0.15 w.%) are shown to be cytotoxic to keratinocytes at higher doses but this level of cytotoxicity is still acceptable if coatings are not swelling rapidly (Figure 5). When deposited on kapton, these coatings are shown to be less cytotoxic to keratinocytes at higher doses. Therefore, an interesting compromise between antifungal effect and cytotoxicity is reached here. Immersion tests in water for 24h showed a weak hydrolysis of some parts on the top of the coatings due to the too low cross-lining ratio of the coating. However, the coating is always covering the whole substrate after the immersion test, ageing test or any other durability test. It can be considered as a coating releasing antimicrobial agent in solution at the same time as matrix molecules, including boric acid. This can explain the high antifungal activity. This dissolution rate is too high for a use over years. The cross-linking ratio needs to be improved for the final applications targeted here. However, these coatings could be interesting for some other applications where both antibacterial and antifungal effects are needed.

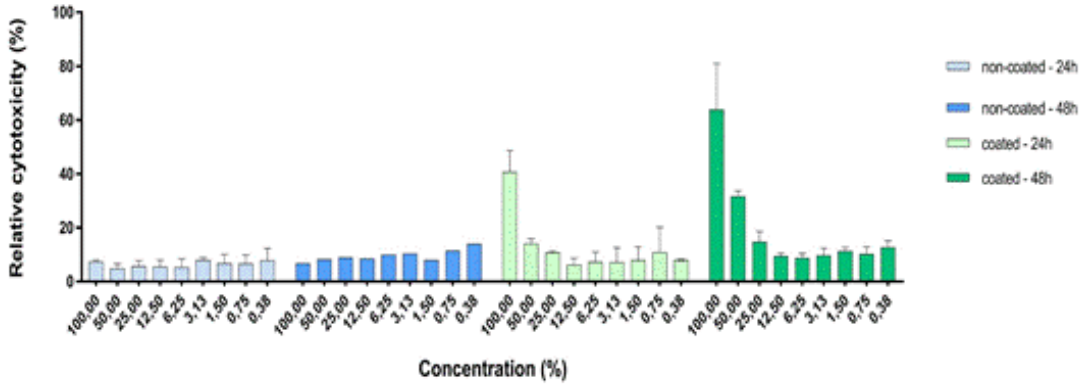

Figure 5. Cytotoxicity (%) on human skin keratinocytes cells with the LDH assay on non-coated stainless steel (blue) and on PVA-based coatings embedding lignin nanoparticles (0.15 w.%) (green)

6 WP3-SOLUTION 4: PVA-based coatings embedding SiO2-Lyzozyme nanoparticles

Here, the same organic matrix is used but the lignin nanoparticles are replaced by silica nanoparticles covalently bonded with lyzozymes (antimicrobial peptides) as shown on the Figure 6. Silica nanoparticles may also reinforce the polymer mechanical properties and durability if present in high quantity enough. ToF-SIMS spectra acquired on these coatings show the presence of PVA and boric acid. Chitosan, silica and lysozymes are not detected. It indicates that these later elements are in very low quantity (<0.5%). XPS confirms these results with PVA as the major compound and show a content of 2 at. % B. The nitrogen N detected in low quantity is due to the addition of N contained in lysozymes, chitosan and APTES used to attach lysozymes to the SiO_2 nanoparticles through the linker glutaraldehyde (Figure 6). Therefore, the antimicrobial effect is mainly due to the presence of boric acid with some (synergetic) effects coming from chitosan and lysozymes for these coatings.

Figure 6. Fabrication of PVA-based coatings embedding Lysozyme-silica nanoparticles

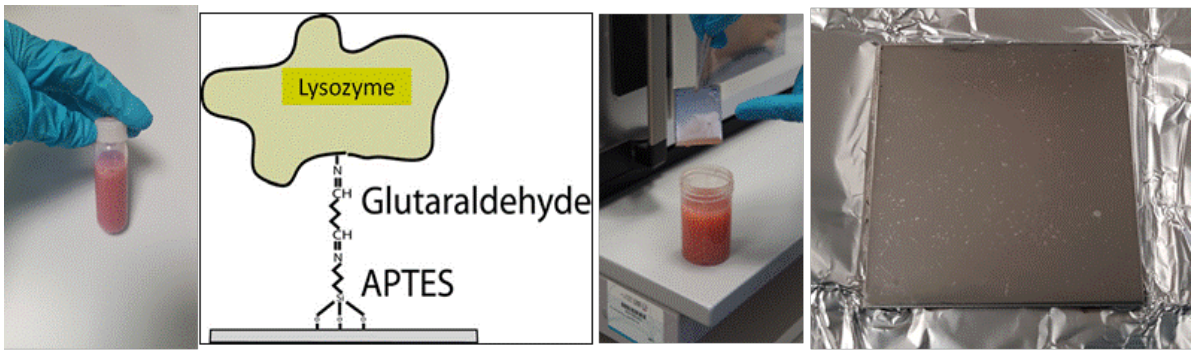

The WCA is about 60° similar to the previous coatings with lignin. As shown on Figure 4 for solution 4 on steel, these coatings show a low activity against on G- bacteria *E. coli* (1.7 log red) and against *S. aureus* (1.0 log reduction) similarly to previous coatings with lignin. The main difference is for *A. niger* with a lower inactivation effect due to the lack of lignin. However, it was shown to be efficient against *C. albicans* fungi (2.7 log reduction). The antimicrobial activity is mainly due to the matrix here and the concentration of silica nanoparticles loaded with lysozyme is too low to generate a significant antimicrobial effect. The durability and cytotoxicity of these coatings are similar to the previous coatings with lignin. A higher cross-linking ratio is needed to decrease the cytotoxicity and improve durability.

7 WP3-SOLUTION 5: Nanopatterned ZnO coatings

Here the idea is to combine the effect of nanopatterns with ZnO antimicrobial effects. LIST solution 5 methodology is based on the deposition of polymer nanostructures by soft lithography, tailoring the of polymer nanostructures by reactive ion etching, coating the polymer nanostructures with a ZnO ultrathin ALD coating and another reactive ion etching step. The nanopatterned ZnO surfaces allow to combine topography effects and chemical effects to inhibit the proliferation of pathogens.

AFM images indicates an average roughness below 20 nanometers mainly due to the rounded pillars present at the surface (Figure 7, left). By analysing AFM images, we confirmed the presence of the ZnO nanopillars in shape of nanotips, with an average height of 10 nm and an average diameter of 40 nm at bottom and a tip diameter of a few nm. The average distance between 2 nanotips is 90 nm (Figure 7, left). The average density of nanopillars is 50 nanopillars/µm. XPS analyses confirm the presence of a very thin film of ZnO and indicate a content of 2 to 9 at.% Zn depending on the position on the samples. WCA is 33-35°due to oxide nature of ZnO and is quite stable with time.

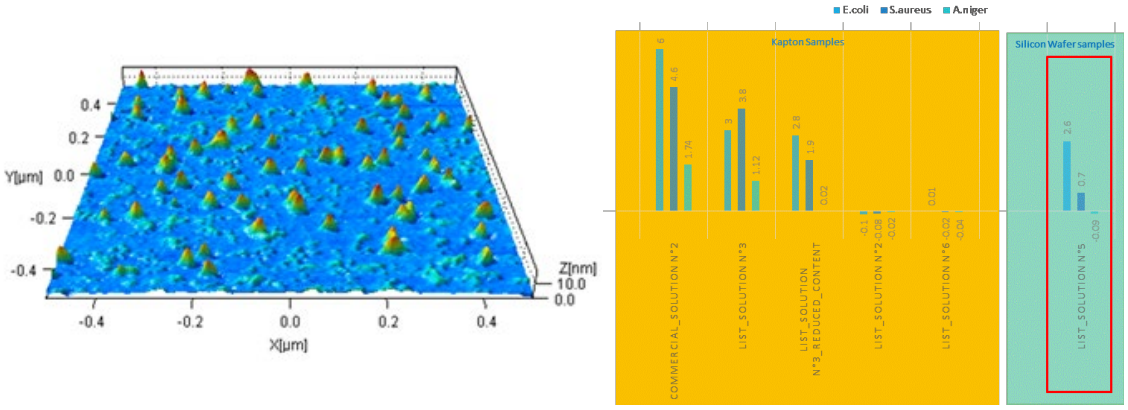

Figure 7. (left) AFM images of nanopatterned ultrathin ZnO films; (right) Inside the red rectangle, antimicrobial Activity, R (logarithm reduction of the number of surviving micro-organisms in cells/cm2) of antimicrobial nanopatterned ZnO coatings deposited on silicon wafer for *E. coli* (left), *S. aureus* (center) and *A. niger* (right)

These coatings show a significant antibacterial effect against G- bacteria *E. coli* (2.6 log reduction) and a very low antibacterial effect against *S. aureus* (0.7 log reduction) when deposited on silicon wafer (Figure 7, right, red rectangle). These coatings do not show an antifungal effect on *A. niger* (Figure 7, right, red rectangle) when deposited on silicon wafer. Human skin keratinocytes cells viability is not affected by both by the non-coated silicon wafer and the nanopatterned ZnO coatings deposited on silicon wafers. Therefore, these coatings are not cytotoxic. The ZnO coatings do not resist to the wipe's test due to low adhesion and/or mechanical strength. Immersion tests in water for 24h showed a release of the coatings in solution as indicated by loss of weight. In conclusion, these coatings showed antibacterial effect against G- bacteria *E. coli* and are not cytotoxic. However, the chemically and mechanical stability issues were not solved whatever the substrate nature (steel or silicon wafer).

.

8 WP4-SOLUTION 1: Highly stable PVA-based coatings with increased concentrations in chitosan and lignin nanoparticles

The same approach than for WP3-solution 3 is used here with the following modifications: PAA and glyoxal has been used to reinforce the mechanical strength and the chemical stability of the coating. Glyoxal is replacing boric acid as cross-linker. Content of chitosan is increased by 1 order of magnitude and concentration of lignin nanoparticles is multiplied by 4 to increase the antibacterial and the antifungal inactivation. Graphene oxide nanoflakes is added to increase antimicrobial properties as well as chemical, thermal and mechanical stability. Also, pre-treatment of the substrates is improved to improve adhesion of coatings on both substrates.
SEM images show a much more homogenous surface, compared with coatings of WP3, due to the use of bar coating deposition processes allowing a better control of thickness and roughness. ToF-SIMS spectra acquired on these coatings show the presence of cross-linked PVA (C2HO+, C2H3O+, C2OH-, C3H3O2-) and chitosan (NH4+, CN-, CNO-). Lignin is hardly detected due to its low concentration. XPS shows a higher C/O ratio compared with WP3 coatings. This is due to the addition of glyoxal and poly (acrylic acid) as well as the important increase of chitosan concentration. Chitosan is now detected with the presence of around 2% of nitrogen. It shows that chitosan content was increased by around 20 to reach a few per cents in concentration. Therefore, antimicrobial effects are mainly due to the presence of chitosan and lignin nanoparticles here. With the optimized PVA-based coatings without graphene oxide, WCA decreases to more hydrophilic values around 30°, whatever the substrates). This is due to the higher content of O-containing groups (chitosan, glyoxal, PAA). When graphene oxide is added (1%), WCA increases to 48°, getting close to the former coatings made in WP3. Wettability properties will not generate an antimicrobial effect by itself.
These coatings show a much stronger antibacterial effect on both G- bacteria *E. coli* (> 6 log reduction, Figure 8, left, in red ellipses) and against *S. aureus* (>5 log reduction, Figure 8, right, in red ellipses) when deposited on kapton with a lignin concentration of 0.7 w.%. Therefore, the change of formulation/composition was very beneficial despite the much lower thickness and slower coating release during immersion (like in antibacterial test). This is due to the increase of chitosan (x 20) and lignin (x5). On steel, the effect of optimised PVA-based coatings is much lower on both *E. coli* (1.2 log reduction) and *S. aureus* (0.9 log reduction) bacteria and slightly lower than WP3 PVA coatings and other coatings.

It not clear yet if this strong influence of the substrate is due to adhesion issues of the coatings on steel or to the fact that the steel reference is releasing antibacterial Cr ions, making the effect of coatings less visible. The same detrimental effect of steel substrate was observed for the other coatings. In conclusion, on kapton, where adhesion is high and no Cr ion is released for the reference substrate, the antibacterial effect is even higher than the reference commercial solutions.

Concerning the fungi *A. niger*, an opposite effect to bacteria ones is observed (Figure 9, left, in red ellipses). On kapton, no effect is detected for optimized coatings. A stronger effect was observed with WP3 coatings. Optimized coatings are much more stable in water and much thinner. Therefore, they do not release enough biocides into the fungi medium to have a significant effect on fungi. Also, no more boric acid is present in the coating, due to its substitution by glyoxal. On steel, surprisingly, the optimized PVA-based coatings show the same inhibitory effect (log reduction of 1,4) than coatings from WP3 (log reduction of 1,6). The effect is still lower than the best commercial coatings (log reduction of 3) but it is considered as a success (log reduction of 1). It is difficult to explain this effect. Maybe a synergetic effect of biocides from the coatings with metal ions from the steel substrate and/or polyethylene imine (PEI) used to improve adhesion of coatings on steel could explain this antifungal effect on steel. Indeed, due to the lower adhesion of coatings on steel, compounds (metal ions, PEI) present at the interface steel-coating could diffuse into the fungal medium and act synergistically to chitosan and lignin.

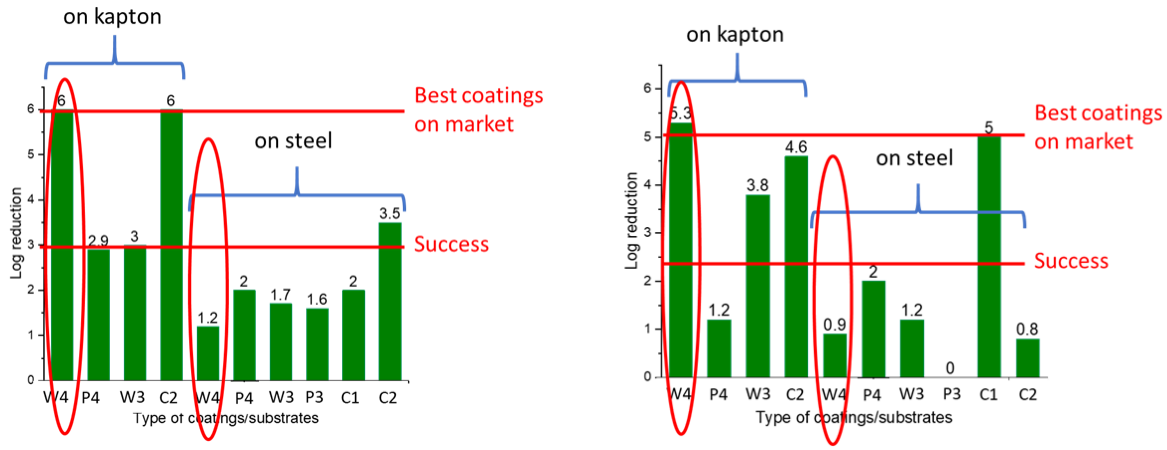

Figure 8. Antimicrobial Activity, R (logarithm reduction of the number of surviving micro-organisms in cells/cm2) of optimized PVA-based coatings embedding lignin nanoparticles for *E. coli* (left, W4, inside red ellipses) and for *S. aureus* (right, W4, inside red ellipses) compared with optimized plasma coatings (P4), former PVA-based (W3) and former plasma-based coatings (P3) and commercial reference coatings Nitropep (C1) and SCS Microresist (C2). The horizontal red lines indicate the R value to consider the coating effective against the bacterial inhibition and the best performance obtained with the current commercial solutions

A new set of antibacterial tests with *Pseudomonas Aeruginosa* bacteria were carried out to simulate more real bacteria adhesion and growth on surfaces. This test indicates a significant reduction (2.6 log. red.) of bacteria adhesion on the optimized PVA-based coatings deposited on kapton after 1h. These results confirmed the previous results with the conventional antibacterial tests. A second test, called biofilm test, shows the efficiency of a coating to inhibit the formation of a biofilm of *P. aeruginosa* in normal conditions (without applying a plate after bacterial medium) and for 14h. In this second test, no effect to inhibit the film growth formation is detected.

Optimized PVA-based coatings embedding lignin nanoparticles (0.7 w.%) are not cytotoxic to keratinocytes by using LDH assay at 24h and 48 hours. Human skin keratinocytes cells viability (MTT assay) decreases slightly to 90% for PVA-based coatings embedding lignin nanoparticles (0.7 w.%) even when 100% of the coating is dissolved in the cell medium (Figure 9, right). In conclusion, the optimized coatings are much less cytotoxic despite they are more active against bacteria. Therefore, the novel PVA-based coatings from WP4 are much more biologically selective than the one tested in WP3.

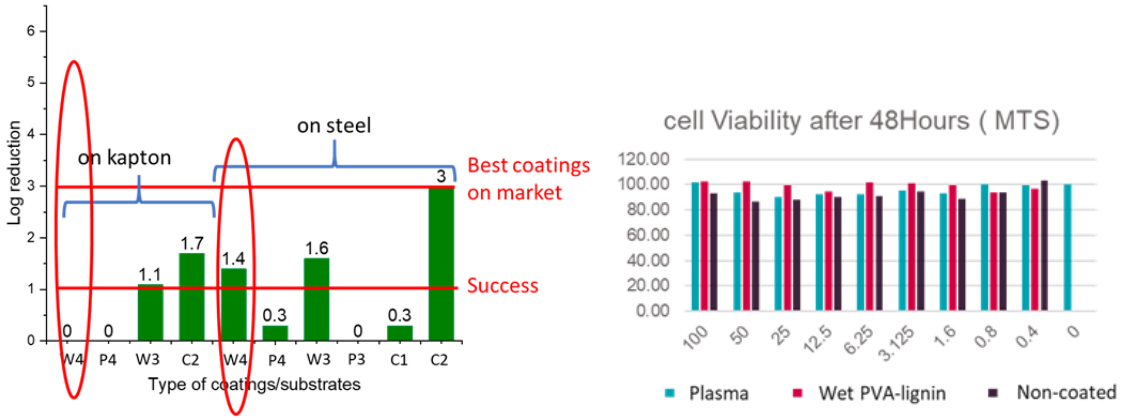

Figure 9. (left) Antifungal Activity, R *(logarithm reduction of the number of surviving micro-organisms in cells/cm2)* of optimized PVA-based coatings embedding lignin nanoparticles for *S. aureus* (W4, inside red ellipses) compared with optimized plasma coatings (P4), former PVA-based (W3) and former plasma-based coatings (P3) and commercial reference coatings Nitropep (C1) and SCS Microresist (C2). The horizontal red lines indicate the R value to consider the coating effective against the bacterial inhibition and the best performance obtained with the current commercial solutions; (right) Human skin keratinocytes cells viability (%) after 48h on non-coated kapton (black), on optimized PVA-based coatings embedding lignin nanoparticles (0.7 w.%) on kapton (red) and on optimized plasma HMDSO coatings embedding lignin on Kapton (blue)

No visible degradation of the coating is detected by applying the wipe's test on both kapton and steel substrates. The optimized coatings are resistant to chlorhexidine, alcohol, and mild mechanical stress. Before going to peel test results, it is important to discuss the effect of different pre-treatment processes on the WCA value i.e. on the cleanliness of both steel and kapton substrates. For kapton, it is shown that whatever the solvent/soap used, the most critical parameter is the 15' UV ozone treatment that is important to get a clean surface (lower WCA values). For steel, where adhesion is more critical, it is clearly show that both cleansing product (alkaline soap, Micro90) and UV ozone treatment are important to get a cleaner surface and then, a higher adhesion as shown below. In WP4, by using the same pre-treatment approach with ethanol/alcohol cleaning and PEI activation, optimized coatings were not adherent. By replacing alcohol by acetone, the coating was much more adherent with only 5-10% of the coating removed instead of 25-35%. This adhesive failure is due to stiffer coatings in WP4 that induces more stress at the substrate-coating interface. In a third step of optimisation, we replace acetone cleaning by an alkaline soap cleaning to remove more organic contamination and the sample passed the adhesion tests without any failure. Immersion tests in water for 24h showed almost no hydrolysis of the coatings thanks to thinner and more stable coatings on both Kapton and stainless steel.
In conclusion, the optimized PVA-based coatings have shown a large progress for all properties except antifungal properties against *A. niger*. The chemical stability/resistance to swelling were improved significantly. Homogeneity of the WP4 coatings was improved significantly with the new bar coating process. However, some inhomogeneities are still present on the edges due to the manual operating mode. These coatings are considered successful to go to the next step, where up-scaling, durability of the antibacterial effect and very low off-gassing will be validated.

9 WP4-SOLUTION 2: Plasma HMDSO-based coatings embedding lignin molecules

The innovative sustainable hydrophobic surfaces have been prepared on both stainless steel and kapton substrates. WP4 LIST plasma solution 2 methodology is based on the application of atmospheric-pressure dielectric barrier discharge plasmas in the torch configuration to polymerize organosilicon monomers embedding lignin sprayed during HMDSO polymerization. It results in a cross-linked, water stable, hydrophobic and highly chemically stable coatings embedding lignin molecules. The PDMS-like plasma structure allows a good compromise between hydrophobicity and chemical stability. Lignin entrapped inside the coatings should not alter the stability of the coatings at low concentration. Optimized HMDSO plasma coatings on steel are very smooth, conformal but they show defects in some places. A lot of nanometric and micrometric particles are present in some parts of the coatings due to formation of small clusters in the gas phase with the addition of lignin. Optimized coatings (WP4) are less homogenous than previous HMDSO-based coatings. It is probably due to the closing of the torch exit with lignin agglomerates and different plasma parameters. One

filter to limit lignin aggregates blocking of the torch exit is needed to limit the formation of these defects. XPS analyses, that are specific to the extreme surface, indicates a slightly higher organic character (-2% at. Si) in optimized coatings with lignin obtained in the torch configuration compared with former HMDSO-based coatings without lignin in WP3. This highly organic character is mainly due to the addition of lignin. Due to the change of plasma configuration, the content of nitrogen is significantly lower (-2.5% at. N) in the optimized coatings. It indicates a lower dissociation of the precursor. It could induce a higher chemical stability but a lower antibacterial effect. However, O content increases (+5% at. O) that can be beneficial to antibacterial properties. The increase of O is mainly due to the addition of lignin. WCA measurements still indicate a hydrophobic behaviour (around 90°).
Antibacterial tests following the procedure **ISO 22196:2011** indicates a significant antibacterial effect on G- bacteria *E. coli* (3 log reduction) considered as successful (Figure 8, left, bars called P4) but a lower effect against *S. aureus* (1.2 log reduction, Figure 8, right, bars called P4) when deposited on kapton. Therefore, the quantity of lignin is probably too low to have higher effect against *S. aureus*.
On steel, the effect of optimised HMDSO-based plasma coatings is lower on *E. coli* (2 log reduction) but higher for *S. aureus* (3 log reduction) bacteria. The addition of lignin mixed with Cr ion release from stainless steel may explain an increase of antibacterial effect on steel. No detrimental effect of steel substrate is observed for the plasma coatings. In conclusion, antibacterial properties were improved significantly by adding lignin in the HMDSO plasma coating. On kapton, this effect is still too low for S. aureus. On steel, effects are considered successful.
Concerning fungi *A. niger*, no effect is observed both on kapton and steel (Figure 9, left, bars called P4). It indicates that lignin is in too low concentration to have a significant effect. Another biocide needs to be added to obtain an effect against *A. niger*. Adhesion and biofilm formation tests with *P. aeruginosa* show that the optimized plasma coatings are not effective to inhibit adhesion and biofilm formation.
Optimized plasma HMDSO coatings embedding lignin molecules (1 w.%) are not cytotoxic to keratinocytes by using LDH assay at 24h and 48 hours. Human skin keratinocytes cells viability (MTT assay) decreases slightly to 95% for plasma HMDSO coatings embedding lignin molecules (1 w.%) even when 100% of the coating is dissolved in the cell medium (Figure 9, right, blue bars). In conclusion, the optimized plasma coatings are not cytotoxic, like the plasma coatings in WP3, despite they are more active against bacteria. Therefore, the novel HMDSO-lignin coatings from WP4 are more biologically selective than the one tested in WP3.
These coatings did not pass the wipe's test on both kapton and stainless steel. Indeed, addition of lignin makes the coatings softer, thicker, and less adhesive. An improvement of pre-treatment and plasma process should lead to successful coatings. On steel, resistance to corrosion was demonstrated in a harsh environment using salt spray corrosion tests for 1 week. Coating opacification occurs after 2 days but no evolution is observed up to 1 week. No more coating failure is observed like for WP3 coatings with a 5% coating delamination. No wrinkling and blistering are observed. It indicates that the coating is resistant to marine environments.
In conclusion, the antibacterial properties of the optimized plasma coatings were improved significantly. Coatings are still chemically stable and hydrophobic. However, homogeneity, mechanical/adhesion strength were decreased by adding lignin and using the torch configuration. Cytotoxicity is still very low. No leaching in water is detected. Optimized plasma coatings improvement allows them to go the next phase where homogeneity, adhesion and antimicrobial properties must be improved in parallel to up-scaling.

10 WP5-SOLUTION 1: Up-scaled PVA-based coatings embedding lignin nanoparticles

SEM images show a quite homogenous surface, even at high magnification, as shown on Figure 10 (left). ToF-SIMS spectra acquired in positive mode on these coatings show peaks distribution characteristic of a polyacrylic acid PAA (*) in the range m/z 300-600, mass differences of 72 Da relative to C3H4O2 monomer are observed between two consecutive peaks (m/z: 365, 437, 509, 581). CxHy+ ions with high intensities indicate the organic structure of the coatings. NH4+ and CH4N+ are characteristic of chitosan present in the coatings. Lignin is hardly detected due to its low concentration or its lack of characteristic peaks. ToF-SIMS spectra acquired in negative mode on these coatings show C2HO-, C2H3O-, CO2H-, C3H3O- and C3H3O2- peaks characteristic of PAA. C2H3O2- and C3H3O2- are characteristic of PVA. CN- peaks are characteristic of chitosan. Detection of alkyl benzene sulfonate is probably due to contaminants from processing. Here also, detection of peaks distribution characteristic of a polyacrylic acid PAA in the range m/z 300-600, mass differences of 72 Da relative to C3H4O2 monomer are observed between two consecutive peaks. Lignin is hardly detected due to its low concentration or its lack of characteristic peaks. Peaks specific to chitosan are detected at 58, 60 and 96 m/z. Here, these peaks can be observed in the coatings due to the concentration of 2%. The FTIR spectrum

obtained on the wet antimicrobial coatings is characteristic of PVA polymers with peaks at 3273, 2914, 1708, 1414, 1320, 1047 and 828 cm^{-1}. These peaks are generally assigned to the O–H stretching vibration of the hydroxy group, CH_2 asymmetric stretching vibration, C=O carbonyl stretch, C–H bending vibration of CH_2, C–H deformation vibration, C–O stretching of acetyl groups and C-C stretching vibration, respectively. The other compounds are not detected due to much lower concentrations. The peak of crystalline PVA at 1142cm^{-1} is not observed that indicates the amorphous nature of PVA. On Figure 10 (right), the XPS spectrum indicates a slightly lower C/O ratio compared with WP4 coatings [RD12]. N content is similar between the optimized and the up-scaled samples. These small variations are due to the lab scale preparation of the formulation, but it does not affect much the properties of the coatings. This elemental composition is representative of PVA-based coatings containing glyoxal, poly (acrylic acid) and chitosan (N). Chitosan is still detected at the same content with the presence of around 2% of nitrogen

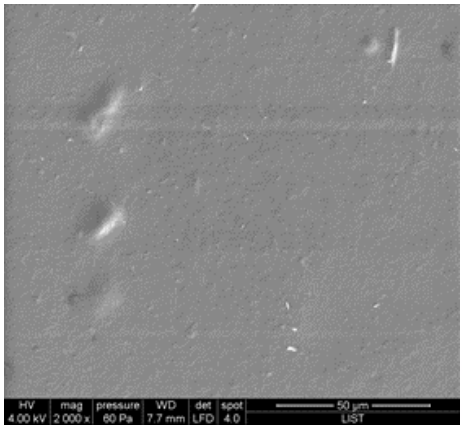

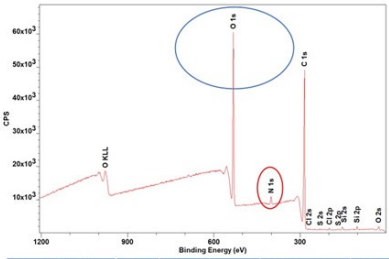

Sample Identifier	C 1s %	Cl 2p %	N 1s %	O 1s %	S 2p %	Si 2p %
WP4	75.4	0.1	1.5	22.1	0.1	0.8
	76.0	0.1	1.6	21.3	<0.1	1.0
	74.1	0.2	1.8	23.0	0.1	0.8

Sample Identifier	C 1s %	N 1s %	O 1s %	Si 2p %
WP5	67.0	2.3	30.1	0.6
	67.2	2.2	30.0	0.7
	67.2	2.2	29.7	0.9

Figure 10. (left) SEM images of up-scaled PVA-based coatings embedding lignin nanoparticles; (right) XPS analyses on PVA-based coatings embedding lignin nanoparticles

Up-scaled coatings (WP5) indicates a similar WCA compared with the former ones containing graphene oxide in WP4 with values around 55°, whatever the substrates.

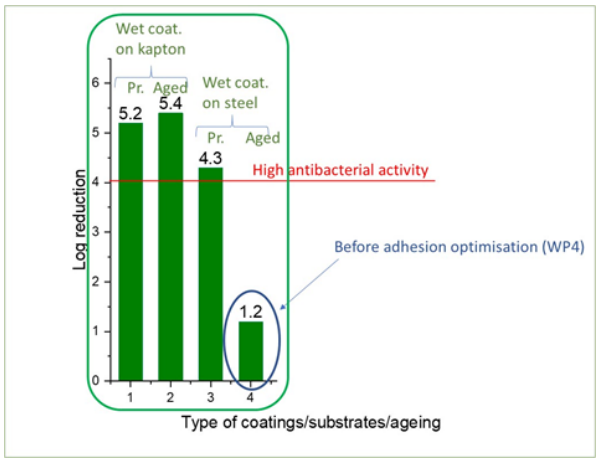

V volume of chamber = 1,47 L

V_{SC} Spacecraft volume = 100 m³

Mass $_{abs}$ Overall absolute amount off-gassed from the item / payload [µg] = Emission in chamber / V

SMAC Spacecraft Maximum Allowable Concentration [µg/m³] listed in NASA-database MAPTIS; in case a value can not be obtained a minimum level of 100 µg/m³ is defined

PSC Projected Spacecraft Concentration based on amount of compound emission in chamber related to spacecraft volume

T $_{ind}$ individual Toxicity value of compound = PSC/SMAC

CAS-Nr.	Substance	Test chamber concentration [µg/m³]	SMAC [µg/m³]	Mass [µg]	PSC [µg/m³]	T ind
1634-04-4	tert-buthylmethylether	27	86.900	0,0398	4,0E-04	4,6E-09
66-25-1	n-hexanal	12	20.000	0,0177	1,8E-04	8,8E-09
64-19-7	acetic acid	115	7.400	0,1693	1,7E-03	2,3E-07
64-17-5	ethanol	953	2.000.000	1,4033	1,4E-02	7,0E-09

T-value = Σ T $_{ind}$

L 3738 FM	T-value =	0,0000003

The acceptance level of the T-value < 0,5 is maintained.

Figure 11. (left) Antibacterial Activity, R *(logarithm reduction of the number of surviving micro-organisms in cells/cm²)* of up-scaled PVA-based coatings embedding lignin nanoparticles for *E. coli* (1-2-3-4, inside green square; Pr. = pristine; Aged = aged coatings). The horizontal red lines indicate the R value to consider the coating highly effective against the bacterial inhibition; (right) Off-gassing test following ECSS-Q-ST-70-29C standard on PVA-based wet coatings deposited on Kapton

Like in WP4, these coatings show a strong antibacterial effect on both G- bacteria *E. coli* (> 5 log reduction, Figure 11, left, col. 1) and against *S. aureus* when deposited on kapton with a lignin concentration of 0.7 w.% and graphene oxide nanoflakes. On steel, the effect of up-scaled PVA-based coatings was improved a lot compared with WP4 on both *E. coli* (4.3 log reduction, Figure 11, left, col. 3) and *S. aureus* bacteria. It is due to a better adhesion on steel. **Concerning aged samples** for 3.5 months simulating more than 5 years of utilization in harsh environment (55°C, 60 % humidity),

results show a high durability of the PVA-based coatings (Figure 11, left, col. 2) with an **intact antibacterial effect** for *E. coli*. In addition to the increased adhesion of coatings on steel substrates, the higher durability of samples in WP5 is also probably favoured by the addition of graphene oxide nanoflakes. In conclusion, on kapton, where adhesion is high, the antibacterial effect is higher than the reference commercial solutions and it can be maintained over years. On steel, adhesion was improved significantly. It leads to stronger antibacterial effects of the optimized PVA-based coatings on steel close to the one observed on Kapton and on the commercial coatings. The durability is shown to be high also on steel substrate for coatings done in WP4 (same results expected on steel because chemical composition is similar). Therefore, the antibacterial properties are validated for the PVA-based coatings (wet approach). All other durability tests demonstrated a good resistance to mechanical and immersion tests as already observed in WP4. Off-gassing results show very low quantities of only 4 VOCs (ethanol, acetic acid, n-hexanal and tert-buthylmethylether) detected (Figure 11, right). It gives a T-value of 3.10^{-7} largely smaller than the critical T-value for acceptance of 0.5. Coatings passed this test thanks to the low quantity of coating deposited and their high stability and adhesion.
In conclusion, the up-scaled PVA-based coatings have shown a large progress for all properties except antifungal properties against fungi. The chemical stability/resistance to swelling were improved significantly. Homogeneity of the WP5 coatings was improved significantly with the bar coating process. However, some inhomogeneities are still present on the edges due to the lab scale operating mode. The maintenance of antibacterial efficiency after long ageing tests is validated. The very low off-gassing for volatile organic compounds is validated following the standard proposed by ESA. The thermal resistance if high for these kinds of antimicrobial coatings. These coatings are therefore considered successful to go for further improvements and up-scaling stages.

11 WP5-SOLUTION 2: Up-scaled HMDSO-based coatings embedding lignin molecules

The same process than for WP4-Solution 2 is used here with the main modification being the 2-layer approach. A bottom layer without lignin and with a pure HMDSO coating, more cross-linked to generate a stronger adhesion on substrate and a second top layer with HMDSO embedding lignin like in WP4, for the antimicrobial activity. Similar morphology, chemical composition, WCA, antimicrobial properties and durability were observed. The only improvement is observed with the wipe tests on Kapton with a higher adhesion of this 2-layer coating. Also, it was demonstrated a low off-gassing following the ESA protocol. Off-gassing results show very low quantities of 7 VOCs detected. It gives a T-value of 1.10^{-7} largely smaller than the critical T-value for acceptance of 0.5. Plasma coatings passed this test thanks to the low quantity of coating deposited and their high stability and adhesion. In conclusion, the antibacterial properties of the optimized plasma coatings were not improved compared with WP4. Only the adhesion on Kapton was improved compared with WP4. Coatings are still chemically stable and hydrophobic. However, mechanical/adhesion strength is still too low due to addition of lignin and use of the torch configuration. Cytotoxicity is still very low. No leaching in water is detected. Improvement of chemical composition and adhesion is still mandatory for going further.